Applied Catalysis B: Environmental 231 (2018) 51–61

Contents lists available at ScienceDirect

Applied Catalysis B: Environmental

journal homepage: www.elsevier.com/locate/apcatb

Kinetic and mechanistic analysis of azo dyes decolorization by ZVI-assisted Fenton systems: pH-dependent shift in the contributions of reductive and oxidative transformation pathways

Jorge A. Donadelli[a], Luciano Carlos[b], Antonio Arques[c], Fernando S. García Einschlag[a,*]

[a] Instituto de Investigaciones Fisicoquímicas Teóricas y Aplicadas (INIFTA), CCT-La Plata-CONICET, Universidad Nacional de La Plata, Diag 113 y 64, La Plata, Argentina

[b] Instituto de Investigación y Desarrollo en Ingeniería de Procesos, Biotecnología y Energías Alternativas, PROBIEN (CONICET-UNCo), Buenos Aires 1400, Neuquén, Argentina

[c] Grupo de Procesos de Oxidación Avanzada, Departamento de Ingeniería Textil y Papelera, Universitat Politècnica de València, Campus de Alcoy, Alcoy, Spain

ARTICLE INFO

Keywords:
ZVI-assisted Fenton
Azo Dyes
pH dependent mechanism
Advanced oxidation processes
Wastewater treatment

ABSTRACT

The chemical decolorization of the azo-dye Acid Black 1 (AB1) by ZVI-assisted Fenton systems was investigated for assessing the relative importance of reductive and oxidative pathways. To this end, system evolution was followed by UV–vis, HPLC, CG–MS, TOC and toxicity measurements. The effects of reaction conditions including initial pH, oxidants (O_2 and H_2O_2) concentrations, ZVI loading, and the presence of SO_4^{2-} were studied. Mechanistic issues were addressed by following H_2O_2, Fe(II), Fe(III) and pH profiles, as well as by performing experiments in the presence of iron-complexing agents (*o*-phenanthroline and EDTA) or reactive species scavengers (2-propanol and DMSO).

Results show that AB1 reduction occurs through heterogeneous processes with moderate to low pH dependent rates, whereas AB1 oxidation is ruled by the Fenton reaction with significantly pH dependent rates. Mechanistic studies demonstrated that AB1 decolorization in ZVI-assisted Fenton systems involves both oxidative and reductive pathways, whose relative contributions significantly change as the initial pH is raised from 3 to 5. In acidic media, AB1 is mostly transformed by oxidative pathways linked to H_2O_2 consumption. In contrast, in circumneutral media, a rather inefficient H_2O_2 consumption leads to similar contributions of oxidative and reductive AB1 transformation pathways. A detailed analysis of the pH dependence of the key reactions involved suggests that the overall system behavior is ruled by a shift in the oxidation mechanism of Fe(II) species, as a consequence of the development of a thigh corrosion layer onto ZVI particles at circumneutral pH values.

1. Introduction

Due to the high quantities of water used in dyeing processes, the textile industry is one of the largest generators of highly polluted liquid effluents. Azo dyes constitute more than 60% of all dyes used, making them the most common synthetic dyes released into the environment [1]. Azo dyes are colored due to the delocalization of electrons in conjugated systems; their structures usually bear one or more azo bonds (−N═N−) that couple aromatic systems containing auxochrome groups such as −OH, $-NH_2$, $-NO_2$, −COOH and/or $-SO_3H$. The environmental impact of these dyes is not only because of its color, but also due to the fact that many azo dyes and their breakdown products (frequently colorless amines) are toxic and/or mutagenic to living organisms [2].

Pollutant removal from water and wastewater may be achieved by biological, physical or chemical methods. Due to their complex structure and recalcitrant nature, azo dyes are difficult to degrade by means of biological methods [2,3]. On the other hand, physical methods, such as flocculation, adsorption and reverse osmosis, are non destructive and simply transfer these pollutants from one phase to another producing a secondary waste that needs to be further treated [2]. Chemical transformation of azo dyes may be accomplished through either oxidative or reductive pathways. Oxidizing agents such as ozone, hydrogen peroxide or Fenton reagent have been frequently used [4], whereas typical reducing agents include sodium borohydride, sodium hydrosulfite [4] and zero valent iron [1,5]. Oxidative methods are capable of transforming both the azo bonds and the aromatic moieties of the conjugated systems. In contrast, decolorization of azo dyes by chemical reduction is

* Corresponding author at: Instituto de Investigaciones Fisicoquímicas Teóricas y Aplicadas (INIFTA, UNLP, CCT La Plata-CONICET), Diagonal 113 y 64, Sucursal 4, Casilla de Correo 16, (B1900ZAA) La Plata, Argentina.
E-mail address: fgarciae@quimica.unlp.edu.ar (F.S. García Einschlag).

https://doi.org/10.1016/j.apcatb.2018.02.057
Received 30 June 2017; Received in revised form 25 December 2017; Accepted 25 February 2018
Available online 27 February 2018

mainly associated with the cleavage of the azo bond.

Fenton methods allow high depuration levels, at mild temperature and pressure conditions, using relatively nonhazardous and easy to handle reactants. These methods are based on the production of highly oxidizing species in the presence of H_2O_2 and ferrous ions (Eqs. (1) and (2)) [6,7]

$$Fe(II) + H_2O_2 \rightarrow [Fe^{III}OH]^{2+} + HO\cdot \quad (1)$$

$$Fe(II) + H_2O_2 \rightarrow [Fe^{IV}O]^{2+} + H_2O \quad (2)$$

It is currently accepted that hydroxyl radicals dominate the oxidation of organic substrates in acidic environments, whereas high valence iron-oxo species (such as ferryl ions) may participate in oxidative pathways at neutral and slightly alkaline pH values [6,8–10].

On the other hand, Zero Valent Iron (ZVI) is a low cost and environmental friendly reducing agent that has been used to remove a wide range of pollutants. Several studies [1,5] have reported the reductive transformation of azo dyes by the use of ZVI as primary electron donor (see Eq. (3) below). ZVI-based technologies may involve a variety of removal pathways that include both chemical transformations (reduction/oxidation) [8,9] and physical processes (adsorption/co-precipitation) [11] whose relative importance may strongly depend not only on the nature of the target pollutant but also on the operating conditions [8]. ZVI particles in contact with water are unstable and corrode spontaneously. Aqueous iron corrosion essentially occurs through an electrochemical process whose anodic half reaction is the production of ferrous species [12].

$$Fe(0) \rightarrow Fe(II) + 2e^- \quad (3)$$

The oxidation of bare Fe(0) in acidic media (pH < 4) is usually linked to the reduction of H^+ [12], whereas the reduction of dissolved O_2 is the major cathodic process at near neutral pH values [12]. The global stoichiometries of the latter processes may be represented by Eqs. (4) and (5)

$$Fe(0) + 2H^+ \rightarrow Fe(II) + H_2 \quad (4)$$

$$Fe(0) + 2H^+ + 1/2O_2 \rightarrow Fe(II) + H_2O \quad (5)$$

The mechanism associated to the production of H_2 involves single electron transfer steps with the formation of adsorbed atomic hydrogen (H·) as intermediate species [13]. On the other hand, the electrochemical reduction of dissolved oxygen is believed to proceed either by a 4 e- process that directly yields H_2O on bare iron [14] (Eq. (5)) or through two consecutive 2 e- reductions, with the formation of H_2O_2 as intermediate on passive iron [8–10,14] (Eqs. (Figure 6) and (7))

$$Fe(0) + 2H^+ + O_2 \rightarrow Fe(II) + H_2O_2 \quad (6)$$

$$Fe(0) + 2H^+ + H_2O_2 \rightarrow Fe(II) + 2H_2O \quad (7)$$

In addition to H^+ and O_2, other species may also act as ultimate electron acceptors. Depending on the composition of the aqueous phase, these species may include Cr(VI), NO_3^-, H_2O_2, Fe(III), nitro-compounds, azo-compounds and even H_2O [12,15].

It should be taken into account that the behavior of ZVI/H_2O systems is conditioned by the fact that Fe(II) may be further oxidized yielding Fe(III). Ferric species are rather insoluble above pH 4 and their precipitation usually leads to the formation of a corrosion layer (CL) onto the surface of ZVI particles [16,17]. The oxidation of Fe(0) initially yields a large array of porous hydroxides which are further transformed into less porous oxides by dehydration [15]. The oxide films should not be considered as rigid layers since they continually undergo both growth and dissolution/flake off processes [15]. Hence, the precise structure of the CL depends on the aqueous phase composition, the hydrodynamic conditions and the contribution of aging processes. Reported corrosion products include ferrous species ($FeO/Fe(OH)_2$), mixed valence iron compounds (Fe_3O_4/GreenRust) and ferric species ($Fe_2O_3/FeOOH/Fe(OH)_3$) [12,17]. Although corrosion layers are microscopically heterogeneous structures that evolve with time and changing reaction conditions [12], they may be considered as stratified films which gradually change form ferrous compounds that dominate the composition of the inner layer (adjacent to the reducing metal surface) towards ferric compounds that dominate the composition of the outer layer (next to the oxidizing species present in the aqueous phase). It is important to highlight that, depending on both its structure and composition, the corrosion layer may substantially decrease both the reactivity [17] and the utilization efficiency [18] of metallic iron. Hence, the investigation of the role of passive layers under different operational conditions is of major concern for practical applications of ZVI [16,18].

Since iron species are continuously released to the aqueous phase in ZVI-based technologies, a number of papers have focused on the degradation of azo dyes in batch systems by using ZVI as source of iron ions in the presence of added H_2O_2 [19,20]. It is important to note that depending on the working conditions (e.g. pH, ZVI loading and the concentrations of both O_2 and H_2O_2), the direct reaction of added H_2O_2 with ZVI (Eq. (7)) may lead to a rather inefficient consumption of hydrogen peroxide in ZVI-assisted Fenton systems [21].

Given the simultaneous occurrence of reductive and oxidative processes in ZVI-assisted Fenton systems, the relative contributions of each pathway may vary with reaction conditions. However, most studies have mainly focused on the transformation and mineralization rates under different operating conditions [19,22–24] and, to the best of our knowledge, several mechanistic issues, concerning the effect of aqueous phase composition and the impact of the corrosion layers on the individual contributions of oxidative and reductive transformation pathways, have not been addressed yet.

In the present work we have investigated the kinetics of Acid Black 1 (AB1) transformation in ZVI/O_2/H_2O_2 systems. For comparison purposes, AB1 treatments under purely reductive conditions (i.e., ZVI/N_2 systems), were also evaluated. The main objectives of this study were: *i*- the evaluation of the relative contributions of reductive and oxidative transformation pathways under different operating conditions, *ii*- the analysis of the impact of the corrosion layer on the kinetics and the efficiency of AB1 decolorization, and *iii*- the assessment of the pH-dependent role of Eq. (7) in ZVI-assisted Fenton systems.

2. Materials and methods

2.1. Reagents

Electrolytic ZVI powder was provided by Anedra (> 98%, BET area of 0.67 m^2/g) and used as received. Acid Black 1 (for microscopy), hereafter AB1 (structure given in Scheme S1, Supp Info), *o*-phenanthroline (97%), KSCN (99%), isopropanol (99.8%), sodium acetate (99.9%) and Na_2SO_4 (99%) were purchased from Anedra. H_2O_2 (perhydrol 30%), H_2SO_4, NaOH were provided by Merck and methanol (pro-analysis, 99.8%) was provided by Cicarelli. All the solutions were prepared using water of Milli-Q grade (Millipore).

2.2. Experimental conditions

Batch experiments were conducted in a 250 ml pyrex® reactor. AB1 solutions were prepared at a concentration of 50 mg L^{-1}. In order to avoid potential interferences in the presence of either organic or inorganic buffers [25] and to properly analyze the correlativity between pH evolution and system behavior [26], it was decided not to use any buffer. The initial pH was adjusted by drop wise addition of 0.1 M H_2SO_4 and/or 0.1 M NaOH, whereas the total ionic concentrations were set by adding 5 mM of Na_2SO_4. Two main groups of experiments were performed: i) predominantly reductive experiments conducted in vessels under continuous N_2 bubbling (hereafter ZVI/N_2 systems), where AB1 solutions were purged with N_2 for 30 min before the addition of

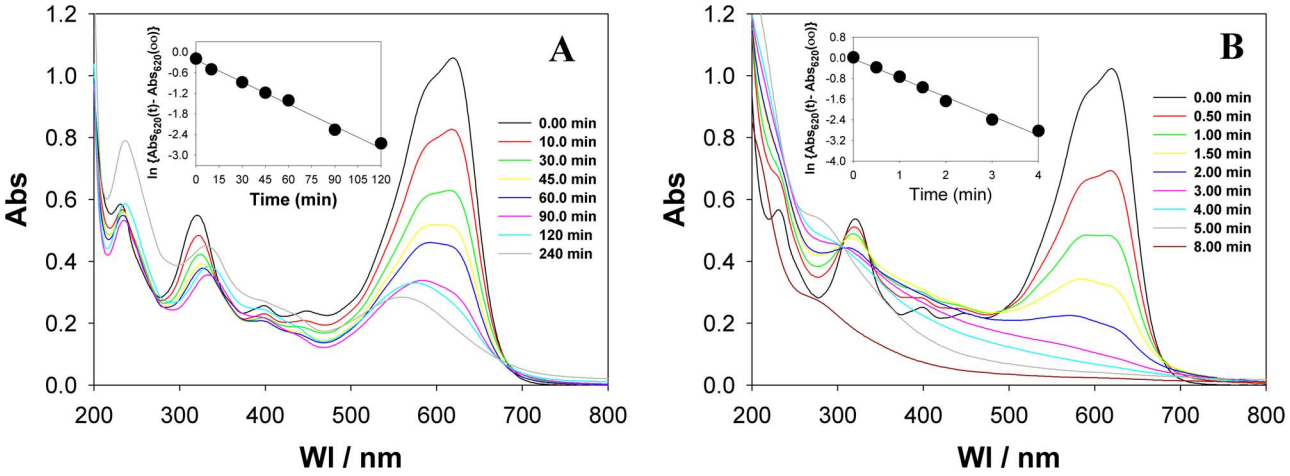

Fig. 1. Time resolved spectra obtained during AB1 decolorization experiments. (A) ZVI/N_2 system. (B) ZVI/O_2/H_2O_2 system with 2.0 mM of H_2O_2. Initial conditions: pH_i 3, ZVI = 0.20 g L^{-1}, $[AB1]_0$ = 50 mg L^{-1}, $[Na_2SO_4]_0$ = 5.0 mM. Insets: observed first order decays obtained using the linear form of Eq. (13).

ZVI powder, and ii) predominantly oxidative experiments in open vessels (hereafter ZVI/O_2/H_2O_2 systems), where H_2O_2 (0.4 mM–8.0 mM) and AB1 were present in the air-saturated aqueous phase before ZVI addition. During experiments performed in the presence of H_2O_2, samples (4 mL) withdrawn at different reaction times were mixed with 1 mL methanol and 3 mL of H_2O to prevent composition changes between sampling and UV–vis or HPLC analyses [27].

All the experiments were carried out at room temperature and under vigorous magnetic stirring (270 rpm). Samples were passed through 0.45 μm cellulose acetate filters before analysis, excluding those designed for assessing Fe(II) and Fe(III) levels. ZVI loadings were in the range 0.04–4 g L^{-1}.

2.3. Analytical techniques

Specific surface area of pristine ZVI particles was determined by N_2 adsorption at 77 K (BET method) using a Micromeritics ASAP 2020 instrument. UV–vis spectra at different reaction times were recorded using a double-beam Shimadzu spectrophotometer (UV-1800). Total organic carbon (TOC) was determined with a Shimadzu apparatus (TOC-VCSH). AB1 concentration measurements were performed by HPLC with a Shimadzu instrument (solvent delivery module LC-20AT, online degasser DGU-20A5, UV–vis photodiode array detector SPD-M20A, column oven CTO-10 A5 VP and autosampler SIL-20AAT) equipped with an Alltech Prevail Organic Acid 5 μm column (RP-C18, 150 mm long × 4.6 mm i.d.). The column temperature was maintained at 25.0 ± 0.2 °C. An isocratic mobile phase composed of 22/78 (v/v) ACN/aqueous buffer ($AcNH_4$) was used with a flow rate of 1 mL min^{-1}. Reaction products were also analyzed using a gas chromatograph GCMS-QP2010S (Shimadzu) equipped with a quadrupole mass analyzer and a Meta.X5 (Teknokroma) column. Before GC analyses, samples were concentrated by solid phase extraction (SPE): 200 mL of sample were eluted through a LiChrolut EN 200 mg (Merck) cartridge; then the reaction products were recovered with 3 mL of methanol. A volume of 10 μl of the concentrated solution was injected in the GC–MS; the injection port was kept at 250 °C and the split ratio was 1:30. During the analysis, the temperature was increased from 60 °C to 250 °C with a 5 °C min^{-1} rate. Fe(II) concentrations were determined by mixing 1.5 ml of sample with 1.5 ml of a solution containing *o*-phenanthroline (6 mM), buffer NaAc (0.5 M, pH = 4.75) and NaF 7 mM, and following the absorbance at 510 nm of the complex formed. The addition of NaF is of particular importance to avoid the formation of Fe(II) by Fe(III) reduction [28]. Both filtered and unfiltered samples yielded, within experimental error, the same Fe(II) concentrations showing that insoluble Fe(II) species are negligible for the studied pH range. Fe(III) levels were determined by following the complex formed with SCN^- in acid medium. Colorimetric assays, performed on samples of known concentrations of iron species, showed that filtration at pH 5 leads to incomplete iron recoveries due to the insolubility of Fe(III) species. Therefore total Fe(III) levels were based on the results obtained from unfiltered samples. H_2O_2 concentration was measured by an enzymatic-colorimetric method employing a commercial kit from Wiener (colestat®) for cholesterol quantization [27]. The bioluminescence of the marine bacterium *V. fisheri* was used to assess the toxicity of the samples. The assays were carried out according to the standardized ISO 11348-3 norm, using lyophilized bacteria (*V. fischeri*, NRRL B-11177, Macherey-Nagel). The standard procedure was employed for reconstitution of the bacteria, using a salty solution. Before analysis, the solutions were neutralized by drop wise addition of NaOH. The luminescence was determined with a Lumifix-Bio-10 (Macherey-Nagel) instrument. Toxicity was determined after 15 min incubation. For colored solutions, readings were corrected by subtracting their absorbance at 490 nm according to the method described by Ashworth et al. [29].

3. Results and discussion

3.1. Comparison of AB1 decolorization in ZVI/N_2 and ZVI/O_2/H_2O_2 systems

3.1.1. Decolorization pathways

Preliminary AB1 decolorization tests were performed with an initial pH of 3.00 (pH_i 3 hereafter) using either N_2 or O_2, both in the presence and in the absence of H_2O_2 (Fig. S1, Sup Info). The experiments performed in the presence of H_2O_2 (i.e., ZVI/N_2/H_2O_2 and ZVI/O_2/H_2O_2 systems) showed much faster AB1 decolorization rates than the ones performed in its absence (i.e., ZVI/N_2 and ZVI/O_2 systems). In contrast, relatively small differences in AB1 decolorization rates were found between ZVI/N_2 and ZVI/O_2 systems, whereas almost no differences were found among kinetic profiles in ZVI/N_2/H_2O_2 and ZVI/O_2/H_2O_2 systems operated with equivalent H_2O_2 concentrations. Therefore, for the present work, the experimental study was mainly focused on ZVI/N_2 systems (i.e., the more reductive conditions) and on ZVI/O_2/H_2O_2 systems (i.e., the more oxidative conditions).

Fig. 1 compares the spectra recorded at different reaction times for the transformation of AB1 solutions in both ZVI/N_2 and ZVI/O_2/H_2O_2 systems. The UV–vis spectra of the untreated AB1 solutions are characterized by one main band in the visible range around 620 nm, and by two bands in the UV region located around 320 and 230 nm, respectively. The visible band is due to an extensive conjugation involving aromatic rings and azo-linkages, whereas the UV bands have been

ascribed to the substituted naphthalene and benzene moieties [30].

For the experiment performed in the absence of H_2O_2 (ZVI/N_2), the absorbance in the range 500–700 nm decreased with time until reaching a plateau with a color removal of around 80% after 120 min. The analysis of the spectral evolution shows an important hypsochromic shift of the visible band (around 60 nm), whereas the main spectral features in the UV region are relatively well conserved (except for a moderate bathochromic shift of less than 20 nm in the band located in the UVA region). This suggests that AB1 decolorization in ZVI/N_2 systems is mainly related to the breakage of azo bonds (i.e., reducing the conjugation extent) with no major structural changes in the aromatic rings. As stated in the introduction, in the absence of added oxidants (such as O_2 or H_2O_2), proton mediated ZVI corrosion produces ferrous ions, hydrogen atoms and hydrogen molecules. Hence, depending on the structure of the target pollutant and the nature of the corrosion layer, ZVI may induce the transformation of reducible groups either by direct electron transfer processes from Fe(0) surface or by indirect pathways involving secondary reductants such as H·/H_2 or Fe (II) species [12,31]. In the case of AB1 reducible groups include the azo bonds and the nitro group [5,21,24], thus the overall stoichiometries of their reductive half reactions may be expressed as

$$\text{R-N = N-R'} + 4e^- + 4\ H^+ \rightarrow \text{R-NH}_2 + \text{H}_2\text{N-R'} \quad (8)$$

$$\text{R-NO}_2 + 6e^- + 6\ H^+ \rightarrow \text{R-NH}_2 + 2\text{H}_2\text{O} \quad (9)$$

It has been reported that the reduction of azo groups on iron surface probably occurs through two successive 2e- transfers yielding hydrazo compounds (R-NH-NH-R') as intermediates [5], whereas the reduction of the nitro group occurs through three successive 2e- transfers with nitroso (−N=O) and hydroxylamine (−NH−OH) compounds as reduction intermediates [32].

In line with the spectral evidence presented in Fig. 1a, aniline and *p*-nitroaniline were among the main products found by GC–MS and HPLC-DAD analyses, thus confirming the reduction of both azo bonds of AB1 in ZVI/N_2 systems. It is worth mentioning that, under purely reductive conditions, HPLC profiles exhibited few and well resolved peaks (Fig. S2A, Sup Info). Interestingly, chromatograms obtained at different reaction times showed an important difference between the evolution of aniline and *p*-nitroaniline. The kinetic profiles of aniline signals initially increased until reaching constant values; whereas *p*-nitroaniline signals showed an initial increase followed by a latter decrease until complete disappearance after 180 min (Fig. S3, Sup Info). The latter results show that aniline is a final reaction product in ZVI/N_2 systems, whereas *p*-nitroaniline is an intermediate reaction product since it bears a nitro group that may be further reduced.

In contrast with the behavior observed in the ZVI/N_2 experiment, a fast and complete decolorization was observed within the first 10 min for the ZVI/O_2/H_2O_2 experiment (Fig. 1b). The presence of H_2O_2 clearly enhanced the decolorization of AB1. Furthermore, a significant loss of the main spectral features of the parent compound is observed in the entire spectral domain, thus indicating substantial structural changes under oxidizing conditions. These results may be explained by taking into account that, in acidic media, highly reactive and rather unselective HO· radicals are produced through the Fenton reaction in the presence of added H_2O_2 (Eq. (1)). In general, HO· radicals may react by abstraction of hydrogen atoms, addition to unsaturated bonds or direct electron transfer reactions [7]. In the case of azo dyes, HO· radicals participate in addition reactions that trigger the oxidation of either azo linkages or aromatic structures.

Two mechanisms, involving either C−N or N=N cleavage, have been proposed for oxidative transformation of azo linkages [33,34]. The initial steps of hydroxyl radical addition to azo moieties and the corresponding primary products may be represented as

$$\text{Ar-N = N-Ar'} + \text{HO}\cdot \rightarrow \text{Ar-N}\cdot\text{-N(OH)-Ar'} \rightarrow\rightarrow \text{Ar-N}\cdot\text{H} + \text{O = N-Ar'} \quad (10)$$

$$\text{Ar-N = N-Ar'} + \text{HO}\cdot \rightarrow \text{Ar}\cdot\text{(OH)-N = N-Ar'} \rightarrow\rightarrow \text{ArOH} + \cdot\text{N = N-Ar'} \quad (11)$$

There is still no general agreement on whether the C−N or N=N bond is attacked first [35] and several oxidation products, including hydroxylamine, nitroso, nitrosoamine and hydroxylnitrosamine compounds, have been reported [36,37]. Further reactions may lead to the release of N atoms as inorganic nitrogen species such as NH_4^+, N_2, NO_2^- or NO_3^-, the latter ones being favored under highly oxidative conditions. Theoretical studies suggest that the N=N bond is broken in preference to the C−N bond, whereas the reaction mechanism involving C−N bond cleavage is mainly associated to the hydrazone tautomer rather than the azo tautomer [35]. Despite each point of attack leads to different reaction mechanisms, from a practical viewpoint, both reaction pathways lead to the decolorization of the visible band.

On the other hand, the addition of hydroxyl radicals to aromatic structures is a well known process that, in the presence of molecular oxygen, results in the hydroxylation of aromatic rings and the formation of hydroperoxyl radicals [27].

$$\text{H}_2\text{Ar} + \text{HO}\cdot + \text{O}_2 \rightarrow\rightarrow \text{HArOH} + \text{HO}_2\cdot \quad (12)$$

After successive hydroxylation steps, aromatic structures may undergo ring opening reactions. Subsequently, further oxidative processes may lead to the complete mineralization of the target pollutants [7].

In line with the evidence presented in Fig. 1b, HPLC chromatograms of samples taken under oxidative conditions showed a much more complex pattern of reaction products than that observed under reductive conditions. Besides those peaks associated with AB1 reduction products, several poorly resolved peaks with relatively small areas were detected (Fig. S2B, Sup Info). The latter behavior is in agreement with the variety of intermediates reported during the course of AB1 degradation in UV/H_2O_2 systems [38] and is a consequence of the largely statistical nature of HO· attack. Likewise, GC–MS analyses evidenced the presence of phenol, *p*-nitrophenol, aniline, *p*-nitroaniline, hydroquinone, resorcinol and *p*-benzoquinone among the reaction products formed at early reaction stages. Despite the presence of aniline and *p*-nitroaniline shows that the reductive cleavage of the AB1 azo bond also takes place in ZVI/O_2/H_2O_2 systems, the much faster decolorization rates observed in the presence of H_2O_2 as well as the formation of phenol and *p*-nitrophenol at early reaction stages indicates that HO· radicals efficiently trigger the oxidative cleavage of azo groups (Eqs. (10) and (11)) [35]. In addition, hydroquinone and resorcinol are typical hydroxylated products formed by the attack of HO· radicals to the aromatic rings of phenol and nitrophenols (Eq. (12)) [27].

3.1.2. Decolorization kinetics

The analysis of the temporal evolution of absorbance values at 620 nm (i.e. the peak wavelength of the AB1 visible band) shows that, for both ZVI/N_2 and ZVI/H_2O_2 systems, the kinetic profiles may be properly described by the following equation

$$A(t) = (A_0 - A_\infty) \times e^{(-k_{obs}.t)} + A_\infty \quad (13)$$

were k_{obs}, A_0, and A_∞ are the observed first order rate constant, the initial absorbance and the residual absorbance at the end of the decolorization process, respectively. The latter equation assumes pseudo first order kinetics and takes into account that decolorization efficiencies may not reach 100%. In general, the residual color is dependent on several factors including the structure of the target dye, the transformation mechanism and the iron dosage.

Several authors have reported that reductive transformations in ZVI systems are mainly surface mediated processes, which may exhibit either pseudo-zero order kinetics or pseudo-first order kinetics with respect to dye concentration [5,22,39]. Moreover, depending the operating conditions such as dye concentration, ZVI loading, pH or mixing intensity, shifts in the reaction orders have been observed [5,22,25,39]. Pseudo zero order kinetics are usually observed at relatively high ratios

of dye concentrations to iron dosages, since under these conditions the saturation of reactive surface sites leads to global decolorization rates that are controlled by site reactivity and independent of dye concentration. In contrast, at low dye concentrations relative to iron dosages usually pseudo first order laws are observed since reaction rates are controlled either by mass transport processes or by the adsorption affinity of the dyes onto reactive surface sites [1,22,39,40].

Taking into account the relative low AB1 concentrations used in the present work and that the pseudo-first order law (Eq. (13)) describes well the decolorization profiles, surface sites saturation seems unlikely and pseudo zero order contributions may be disregarded. Given the observed differences in the final decolorization values obtained under different experimental conditions, the apparent first order decay constants were calculated by non linear regression analysis. For the experiments conducted at pH_i 3 (Fig. 1), a much higher k_{obs} value was obtained in the presence of H_2O_2 (i.e., $k_{obs,ZVI/N2} = 0.022 \pm 0.001\ min^{-1}$ and $k_{obs,ZVI/O2/H2O2} = 0.74 \pm 0.03\ min^{-1}$). Consequently, although reductive pathways cannot be completely neglected, the large difference in the apparent rate constants suggests that oxidative pathways are dominant in $ZVI/O_2/H_2O_2$ systems at pH_i 3.

3.1.3. Analysis of pH evolution

Inspection of pH profiles obtained in ZVI/N_2 and $ZVI/O_2/H_2O_2$ systems reveals that, in line with results reported by other authors [8,21,22,25,32,41], pH values increased with reaction time (Fig. S4, Sup Info). This behavior may be ascribed to the significant contribution of ZVI-mediated proton reduction (Eq. (4)) under both reductive and oxidative conditions. The latter hypothesis is supported by the fact that, under the conditions tested, the initial slopes of pH increase (Fig. S4) show little dependence on the presence of H_2O_2. However, after the initial reaction stages the rate of pH increase in the $ZVI/O_2/H_2O_2$ system is lower than that of the ZVI/N_2 system. After 90 min, both pH profiles reached relatively stationary values of about 7.0 and 6.0, in the absence and in the presence of oxidants, respectively. The latter difference may be explained by taking into account that the formation of Fe(III) species under oxidizing conditions yields H^+ through hydrolysis reactions thereby slowing the pH increase associated to ZVI corrosion. It is worth mentioning that pH increases dependent on reaction conditions were previously reported for similar systems [8,22,23,42].

3.2. Effects of operating conditions

In order to analyze the impact of the operating conditions on the AB1 transformation in both ZVI/N_2 and $ZVI/O_2/H_2O_2$ systems, we have studied the dependence of k_{obs} on ZVI dose and aqueous phase composition.

3.2.1. ZVI loading

Fig. 2 shows the effect of ZVI loadings on k_{obs} values obtained for AB1 decolorization in ZVI/N_2 and $ZVI/O_2/H_2O_2$ systems. In line with the results presented in the previous section, much higher decolorization rates were observed in the presence of H_2O_2 for all ZVI loadings. In addition, while no more than a 92% of Abs_{620nm} removal was reached in ZVI/N_2 systems after 120 min, a complete decolorization was observed in $ZVI/O_2/H_2O_2$ systems for all ZVI doses during the first 40 min. Despite color removal in ZVI/N_2 systems was not complete, higher iron loadings led to lower residual color (Fig. S5, Supp Info), according to previously reported results [1].

Inspection of Fig. 2 profiles shows that, in both systems, k_{obs} values increase with ZVI dose. However the observed plots are not linear and the slopes decrease upon increasing ZVI loadings, this effect being much more evident in the presence of H_2O_2. Similar trends have been reported for the transformation of both organic and inorganic pollutants in ZVI-based treatments conducted either in the presence or in the absence of added oxidants [20,23,26,43]. The linear increase of k_{obs} values observed in ZVI/N_2 systems at low iron doses is usually explained by assuming that reactive site concentration increases proportionally with ZVI loading [26,44]. Under this hypothesis, rate constants normalized by surface area (k_{SA}) have been proposed as more general descriptors of Fe(0) reactivity than k_{obs} values [44]. However, at high doses of granular iron, significant deviations from the latter linear correlation have been frequently observed in batch systems [44], thus indicating that reductive mechanisms are more complex than currently envisioned [44].

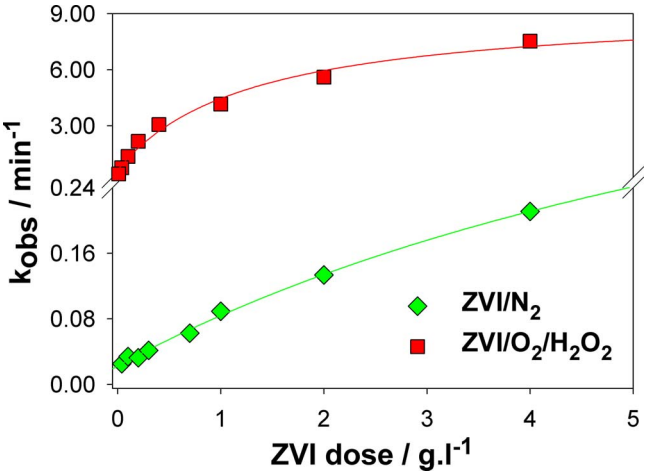

Fig. 2. Effect of ZVI loading on AB1 decolorization rate constants for ZVI/N_2 systems and $ZVI/O_2/H_2O_2$ systems with 2.0 mM of H_2O_2. $[AB1]_0 = 50\ mg\ L^{-1}$, $[Na_2SO_4]_0 = 5.0$ mM, pH_i 3.

Several factors may contribute to the observed curvature at high iron loadings in ZVI/N_2 systems (Fig. 2). These factors include: *i)* a shift from mass-transfer-limited reaction kinetics at low ZVI loadings to kinetics limited by surface reaction rates at high iron doses [44]; *ii)* a decrease in ZVI reactivity due to enhanced passivation associated to faster increases of both pH and Fe(II) levels at higher ZVI loadings [44]; and *iii)* a decrease in the number of available reactive surface sites per gram of ZVI due to aggregation of iron particles at high doses [1]. On the other hand, despite the latter factors may play a role in $ZVI/O_2/H_2O_2$ systems, the higher curvature observed in the presence of H_2O_2 at relatively lower doses clearly suggests that other processes compete with AB1 oxidation pathways as iron dose is increased. Since dye oxidation in acidic media is triggered by HO· radicals produced through Eq. (1), it has been proposed [43] that the scavenging of HO· radicals by Fe(II) (Eq. (14)) competes with dye oxidation due to the increase of Fe(II) levels released by corrosion at high ZVI doses

$$Fe(II) + HO\cdot \rightarrow [Fe^{III}OH]^{2+} \quad (14)$$

However, in addition to the latter process, an important consumption of H_2O_2 by direct reaction with ZVI (Eq. (7)) certainly plays a negative impact on the overall dye decolorization rates at high iron doses. The contribution of ZVI oxidation by H_2O_2 should not be overlooked since, as will be shown in Section 3.4, the overall fraction of H_2O_2 reacting with ZVI is strongly dependent on the reaction conditions. To the best of our knowledge, the importance of the latter reaction in ZVI enhanced Fenton systems has not been properly addressed.

3.2.2. Aqueous phase composition

Several authors reported that both pH and dissolved salts play significant roles on the rates of ZVI corrosion and dye removal [1,3,20,22]. In addition, high Na_2SO_4 concentrations are usually found in dye containing effluents [3]. Therefore, in order to evaluate the effects of these variables on both the decolorization kinetics and the transformation pathways of AB1 under different conditions, both ZVI/N_2 and $ZVI/O_2/H_2O_2$ experiments were performed varying the initial pH from 3.00 to 6.00, either in the presence or in the absence of Na_2SO_4 (Fig. 3).

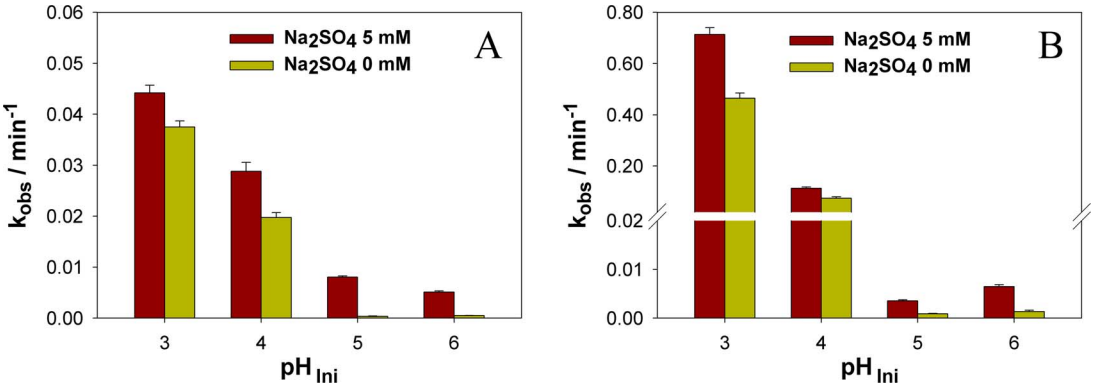

Fig. 3. Effect of initial pH and added Na_2SO_4 on AB1 decolorization rate constants. (A) ZVI/N_2 systems. (B) ZVI/O_2/H_2O_2 systems with 2.0 mM of H_2O_2. Initial conditions: [ZVI] = 0.20 g L^{-1}, [AB1] = 50 mg L^{-1}.

For both ZVI/N_2 and ZVI/O_2/H_2O_2 systems, k_{obs} values are significantly higher for the tests conducted at pH_i values of 3 and 4 (hereafter acidic media) than those obtained at pH_i values of 5 and 6 (hereafter circumneutral media). Similar trends have been reported for the ZVI-mediated decolorization of azo dyes under either reductive or oxidative conditions [1,22]. It is well established that iron reactivity slows down with increasing pH due to the presence of a passive layer of iron oxy-hydroxides on ZVI surface [12,26,45]. Hence, iron passivation may inhibit key processes associated with AB1 decolorization through either reductive pathways or oxidative pathways.

Inspection of Fig. 3 shows that the presence of Na_2SO_4 (5.0 mM) in the aqueous phase enhanced AB1 decolorization rates in both ZVI/N_2 and ZVI/O_2/H_2O_2 systems. The observed enhancement of AB1 removal in the presence of Na_2SO_4 is in contrast with the results reported by Fan et al. concerning the reduction of Methyl Orange in ZVI/N_2 systems [3], and those reported by Weng et al. who found an inhibitory effect of sulfate on Reactive Black 5 decolorization [19]. However, no effect of sulfate was found on Direct Blue 15 oxidation in a ZVI/H_2O_2/ultrasound system [20], whereas the ZVI-mediated reduction of 2,4-dinitrotoluene was a notably enhanced in the presence of SO_4^{2-} [46]. Moreover, Yin et al. reported an enhancement of nitrobenzene reduction that was dependent on sulfate concentration [39]. Hence, the effect of dissolved salts on the removal of azo dyes in the presence of ZVI may be dependent on the dye structure as well as on the nature of the supporting electrolyte and the operating conditions.

The analysis of k_{obs} values indicates that, under our experimental conditions, the relative enhancement of AB1 decolorization rates due to the presence of added SO_4^{2-} is particularly important for the higher pH values tested. In order to evaluate the role of SO_4^{2-} anions under our experimental conditions, additional tests were performed using $NaClO_4$ for adjusting the ionic concentration in the aqueous phase. The profiles obtained in the presence of $NaClO_4$ matched with those observed in the absence of added salts (data not shown), indicating that reaction rates are not controlled by solution's conductivities under the studied conditions. The latter result as well as the strong decrease in the decolorization rates observed at circumneutral pH values suggest that added SO_4^{2-} leads to an increase of granular iron reactivity by removing iron oxides and hydroxides from the iron surface [39], the effect being more pronounced for conditions where an important passivation of ZVI surface is expected [12,17,20].

The results presented in Fig. 3a show that, in the presence of added SO_4^{2-}, a decrease of about two orders of magnitude in the initial concentration of H^+ results in a relatively modest decrease of k_{obs}, thus suggesting that for ZVI/N_2 systems the AB1 transformation mechanism remains unchanged within the analyzed pH range. On the other hand, a different behavior is observed for ZVI/O_2/H_2O_2 systems since, in the presence of oxidants (i.e., O_2/H_2O_2), the decolorization rate is decreased about 240 times upon changing pH_i from 3 to 5 (Fig. 3b). Moreover, in strong contrast with the differences observed in acidic media, k_{obs} values recorded in circumneutral media for ZVI/O_2/H_2O_2 systems are similar to those recorded for ZVI/N_2 systems.

3.3. Investigation of Fe(II), Fe(III) and H_2O_2 profiles

In order to assess some mechanistic aspects of both ZVI/N_2 and ZVI/O_2/H_2O_2 systems, the concentration profiles of Fe(II), Fe(III) and H_2O_2 were measured under different experimental settings. It is important to take into account that, as stated in the introduction, corrosion layers evolve with time and changing reaction environments. Therefore, depending on operating conditions such as mixing rate, scouring rate, pH and the presence of depassivating agents, iron cations may be released into the solution phase as dissolved or particulate species through either dissolution or flake off processes [12,16,18]. Given the complexity of these processes, the levels of dissolved or particulate Fe(II)/Fe(III) species released into the aqueous phase (hereafter released iron) cannot be straightforward correlated with Fe(0) corrosion rates. However, the study of the rates of iron release may help to understand the role of the corrosion layers on the decolorization trends.

3.3.1. ZVI/N_2 systems

Fe(II) measurements in the ZVI/N_2 experiment started at pH_i 3 showed a concentration of released Fe(II) of around 0.4 mM after 120 min (Fig. S6, Sup Info). In contrast, for the experiment started at pH_i 5, the total concentration of Fe(II) measured after 120 min was two orders of magnitude lower than that observed at pH_i 3 (Fig. S6, Sup info). For both initial pH conditions, Fe(III) profiles did not show significant features since their levels remained almost constant and below 0.03 mM. These results suggest that, in the absence of O_2, the oxidation of ZVI surface is mainly ruled by the concentration of protons (Eq. (4)) and that the plateau reached by Fe(II) concentrations in the experiment preformed with pH_i 3 is mainly connected with the increase of the solution pH as reaction progresses (Fig. S4, Sup Info).

In light of the high Fe(II) concentration produced in the ZVI/N_2 system started at pH_i 3, additional experiments were performed in order to test whether the reduction of AB1 azo bonds was induced by the presence of soluble Fe(II) species. Therefore, two solutions containing $FeSO_4$ (1.0 mM) and AB1 (50 mg L^{-1}) were left in the dark for 120 min at pH_i 3 and 5, respectively. In both cases, no changes of AB1 concentration were observed proving that dye reduction by soluble Fe(II) can be discarded within the experimental range analyzed and confirming that AB1 reduction is a surface mediated reaction.

3.3.2. ZVI/O_2/H_2O_2 systems

Fig. 4 compares the profiles of released Fe(II) and Fe(III) species recorded for ZVI/O_2/H_2O_2 systems with pH_i values of 3 and 5. The presence of O_2 and H_2O_2 significantly enhanced ZVI oxidation since the

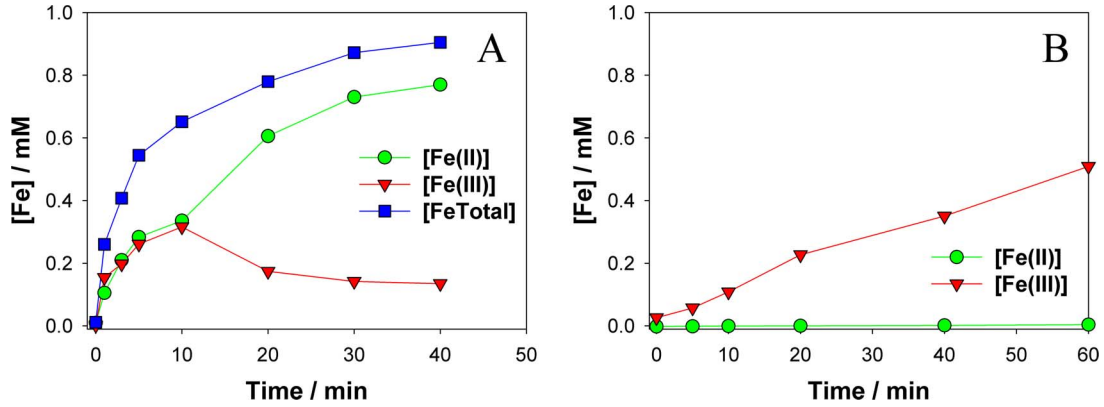

Fig. 4. Fe(II) and Fe(III) profiles in ZVI/O_2/H_2O_2 systems started at pH_i 3 (A), and at pH_i 5 (B). Initial conditions: $[AB1]_0$ = 50 mg L^{-1}, $[H_2O_2]_0$ = 2.0 mM, $[Na_2SO_4]_0$ = 5.0 mM, ZVI = 0.20 g L^{-1}.

recorded total iron levels, defined as $[Fe^{TOT}]$ = [Fe(II)] + [Fe(III)], were clearly higher than those previously discussed for ZVI/N_2 systems.

The profiles obtained in the ZVI/O_2/H_2O_2 experiment started in acidic media (Fig. 4a) show that both Fe(II) and Fe(III) levels increased during the first 10 min. However, after 10 min, a decrease of Fe(III) is observed. This behavior can be rationalized by taking into account that, in acidic media, Fe(III) production is mainly ruled by the presence of H_2O_2 (Eq. (1)) because Fe(II) oxidation by O_2 is negligible below pH 5 [47]. Since H_2O_2 was rapidly depleted within the first 10 min (see Fig. 5 below), at longer reaction times Fe(III) production stopped and Fe(III) levels began to decrease, most likely through a ZVI-mediated reduction whose overall stoichiometry is shown in Eq. (15) [1,23,41].

$$Fe(0) + 2\ Fe(III) \rightarrow 3\ Fe(II) \quad (15)$$

After the first 10 min, Fig. 4a profiles show a high correlation between the decrease of Fe(III) levels and the increase in the rate of Fe(II) production. Moreover, once Fe(II) oxidation is exhausted due to the complete depletion of H_2O_2, Fe(II) levels increase faster than total iron levels and simple calculations show that more than 75% of the decrease in Fe(III) levels can be attributed to the contribution of reaction (15).

On the other hand, Fig. 4b reveals that, for the experiment conducted at pH_i 5, almost all the iron released is found as Fe(III), the levels of Fe(II) being at least two orders of magnitude below those observed at pH_i 3. It is important to note that, despite Fe(II) oxidation by O_2 may be considered negligible in acidic media, for the experiments conducted at circumneutral pH values Fe(II) may certainly be oxidized to Fe(III) by dissolved oxygen. The overall stoichiometry of the latter process may be presented as

$$Fe(II) + ¼\ O_2 + H^+ \rightarrow Fe(III) + ½\ H_2O \quad (16)$$

From a kinetic viewpoint, Fe(II) transformation to Fe(III) by O_2 is a complex process, with an apparent rate constant that increases almost two orders of magnitude as pH is shifted from 5.5 to 6.5 [47]. In addition, it has been reported that the presence of iron oxides may accelerate the oxidation of ferrous iron by oxygen [9] and that the relative contribution of the heterogeneous reaction increases with decreasing pH [28]. Hence, the oxidation of Fe(II) through the overall process represented by Eq. (16) may be quite important for ZVI/O_2/H_2O_2 systems operated in circumneutral media (Fig. 4B). In order to get further insight into the pH-dependent role of dissolved oxygen we have studied the pH profiles in ZVI/N_2 and ZVI/O_2 systems (Fig. S7, Sup. Info). Results show that in acidic media the rate of proton consumption in ZVI/O_2 systems is faster than that observed in ZVI/N_2 systems suggesting an important participation of dissolved oxygen in the oxidation of ZVI through Eq. (5). In contrast, for the experiments initiated at circumneutral pH values the opposite trend is observed. The latter behavior suggests the participation of dissolved oxygen in Fe(II) oxidation, as ferric species formed through R16 subsequently undergo fast hydrolysis reactions that release H^+ and delay the pH increase.

Fig. 4 also shows that given the high concentrations of Fe(II) released into the aqueous phase in acidic media (Fig. 4a), an important fraction of the Fe(II) produced by ZVI corrosion is available for its oxidation trough the Fenton reaction (Eq. (1)). In contrast, at circumneutral pH values the scarce release of Fe(II) to the aqueous phase (Fig. 4b) hinders the participation of the Fenton reaction. It is worth mentioning that, as the initial pH is raised from 3 to 5, the substantial decrease of soluble Fe(II) levels in solution closely matches the decline of k_{obs} values shown in Fig. 3, thus suggesting that the overall rate of AB1 decolorization is strongly correlated with the occurrence of the Fenton reaction.

As expected, the change in the evolution of Fe(II) species upon increasing the working pH impacts on H_2O_2 concentration profiles that show a much faster decay in acidic media than in circumneutral media (Fig. 5). However, despite aqueous phase concentrations of Fe(II) were reduced by more than two orders of magnitude, the apparent first order rate constants for H_2O_2 decay only decreased by about one order of magnitude (i.e. $k_{H_2O_2,pH_i3}$ = 0.319 min^{-1} and $k_{H_2O_2,pH_i5}$ = 0.020 min^{-1}), thus suggesting the contribution of an additional H_2O_2 consumption pathway different from the Fenton reaction. This behavior indicates that the relative contribution of ZVI oxidation by H_2O_2 (Eq. (7)) increases as the initial pH is shifted from acidic to circumneutral values. Moreover the comparison of normalized AB1 and H_2O_2 profiles (Fig. S8, Sup Info) shows that in acidic media the decay timescales of dye and hydrogen peroxide are closely linked, whereas under circumneutral conditions H_2O_2 consumption is essentially decoupled from AB1 transformation.

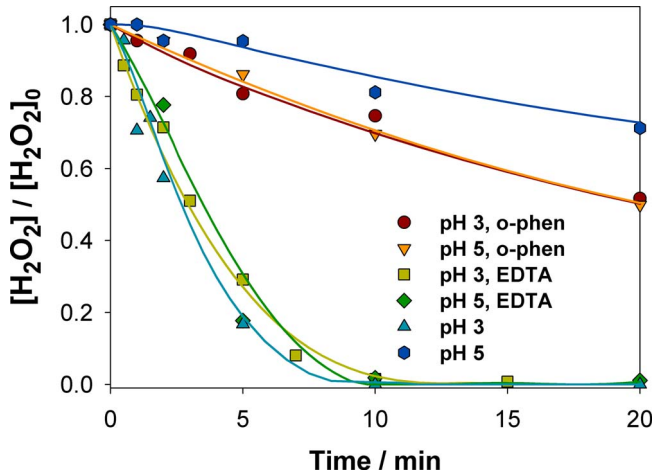

Fig. 5. Comparison of H_2O_2 profiles obtained using different aqueous phase compositions. $[AB1]_0$ = 50 mg L^{-1}, $[H_2O_2]$ = 2.0 mM, [EDTA] or [*o*-phenanthroline] = 3.0 mM, $[Na_2SO_4]_0$ = 5.0 mM, [ZVI] = 0.20 g L^{-1}.

3.4. Kinetic profiles in the presence of additives

Additional experiments were performed in the presence of different additives in order gain insight concerning the effect of the working conditions on: *i*- the role of the corrosion layer, *ii*- the contribution of Eq. (7), and *iii*- the relative contribution of oxidative/reductive AB1 decolorization pathways. The additives were selected in an attempt to selectively influence specific factors affecting the reaction mechanisms and include iron-complexing agents (i.e., ortho-phenanthroline and EDTA) as well as reactive species scavengers (i.e., 2-propanol and DMSO).

3.4.1. Addition of iron-complexing agents

Ortho-phenanthroline is a strong Fe(II)-complexing agent that facilitates the dissolution of insoluble Fe(II) species and also prevents the production of Fe(III) even in the presence of strong oxidants such as O_2 or H_2O_2 [48]. Control experiments performed in the presence of 3 mM of *o*-phenantrholine have shown a complete inhibition of the Fenton reaction for 1.0 mM of Fe(II) and 0.8 mM of H_2O_2 solutions. On the other hand, EDTA is capable of forming highly stable Fe(III) complexes thus preventing the formation of ferric precipitates onto ZVI surface but allows the oxidation of Fe(II) species [45]. Taking into account the conditional stability constants estimated for the latter complexes at pH 3 and pH 5 (Table S1, Sup Info), it can be assumed that in the presence of *o*-phenantrholine iron species are stabilized as the soluble $[Fe^{II}(o\text{-phen})_3]^{2+}$ complex, whereas in the presence of EDTA iron species are stabilized as the soluble $[Fe^{III}EDTA]^{1-}$ complex.

The presence of *o*-phenanthroline significantly increased the levels of released iron at acidic and circumneutral pH values in both ZVI/N_2 and ZVI/O_2/H_2O_2 systems (Fig. S9, Sup Info). Likewise, concentrations of released iron were also enhanced in the presence of EDTA (data not shown). The initial rates of iron release, defined as $r_{Fe}^{Tot} = (d[Fe^{TOT}]/dt)_{Ini}$, under different conditions both in the presence and in the absence of *o*-phenanthroline are compared in Table 1.

The addition of *o*-phenanthroline causes a much more pronounced effect for the experiments conducted at circumneutral pH values because the importance of the CL is enhanced as pH is increased. The results obtained at pH_i 5 in ZVI/N_2 systems demonstrate that the corrosion layer exerts a dramatic effect on the system behavior, r_{Fe}^{Tot} being about 240 times smaller in the absence than in the presence of *o*-phenanthroline. On the other hand, at pH_i 5 in ZVI/O_2/H_2O_2 systems the effect of *o*-phenantroline is less pronounced, since r_{Fe}^{Tot} is only enhanced by a factor of about 20. The latter result can be explained by considering that H_2O_2, due to its strong oxidative and corrosive activity, enhances ZVI reactivity by producing an intensive etching of particle surfaces [16].

The values presented in Table 1 reveal that, in the absence of *o*-phenanthroline, H_2O_2 moderately increased r_{Fe}^{Tot} (i.e. about 3 times) at pH_i 3 but significantly enhanced r_{Fe}^{Tot} (by a factor of about 30) at pH_i 5, suggesting that the relative contribution of ZVI oxidation by H_2O_2 (Eq. (7)) is much smaller in acidic than in cricumneutral media. In contrast, in the presence of *o*-phenanthroline the ratio $r_{FeO2/H2O2}^{Tot} / r_{FeN2}^{Tot}$ is independent of the initial pH. Taking into account that the additive not only blocks the Fenton reaction (leaving Eq. (7) as the unique H_2O_2 consumption pathway) but also exerts a depassivating effect, the latter result suggests that the reactivity of H_2O_2 towards bare ZVI cannot be strongly pH dependent.

Table 1
Initial rates of release of iron species into the aqueous phase.

	o-phen	$r_{FeZVI/N2}^{Tot}$ /mM min^{-1}	$r_{FeZVI/O2/H2O2}^{Tot}$ /mM min^{-1}
pH_i 3	Absent	5.8 (± 0.7) × 10^{-2}	1.7 (± 0.2) × 10^{-1}
pH_i 5	Absent	3.1 (± 0.4) × 10^{-4}	8.3 (± 0.3) × 10^{-3}
pH_i 3	Present	2.5 (± 0.1) × 10^{-1}	5.8 (± 0.5) × 10^{-1}
pH_i 5	Present	7.4 (± 0.3) × 10^{-2}	1.7 (± 0.1) × 10^{-1}

It is worth mentioning that, under all conditions tested, r_{Fe}^{Tot} values decrease with increasing pH. In the absence of depassivating agents, r_{Fe}^{Tot} values are much lower at pH_i 5 than those observed at pH_i 3, thus suggesting that a significant fraction of the iron cations formed by ZVI corrosion becomes "trapped" within the CL at circumneutral pH values. This hypothesis is further supported by the H^+ decay profiles recorded in ZVI/N_2 systems (Fig. S7, Sup. Info), since r_{Fe}^{Tot} values decrease by more than two orders of magnitude but the absolute rates of H^+ consumption decrease only by a factor of about 20 as pH_i is increased from 3 to 5. In contrast, when *o*-phenanthroline is added, r_{Fe}^{Tot} values are much less dependent on the initial pH, the relative enhancement in going from pH_i 5 to pH_i 3 being moderate and rather independent of the presence or absence of H_2O_2.

Additional experiments were performed to evaluate the effects of *o*-phenantroline and EDTA on the kinetic profiles of H_2O_2 consumption in both acidic and circumnetural media (Fig. 5). Interestingly, in clear contrast with the behavior observed in additive-free systems, in the presence of each additive the H_2O_2 decay profiles were practically independent of the initial pH.

Analysis of Fig. 5 shows that, as expected, at acidic pH values the presence of *o*-phenanthroline substantially reduces H_2O_2 consumption by inhibiting the Fenton reaction (Eq. (1)), leaving Eq. (7) as the unique H_2O_2 consumption pathway. The analysis of the initial rates obtained with and without *o*-phenantrholine under acidic conditions shows that about 89% of H_2O_2 consumption involves pathways triggered by Eq. (1), whereas only 11% of H_2O_2 reacts with ZVI through Eq. (7).

In contrast, at pH_i 5 the consumption of H_2O_2 is faster in the presence of *o*-phenantrholine than in its absence. This opposite behavior can be explained by taking into account that the depassivating effect exerted by *o*-phenantrholine enhances the reaction of H_2O_2 with ZVI (Eq. (7)), and also that the inhibition of Eq. (1) due to the presence of *o*-phenanthroline has a negligible impact on H_2O_2 profile since the contribution of Fenton processes in additive-free systems at pH_i 5 is rather low (see Section 3.4.2). Noteworthy, upon addition of *o*-phenantrholine the decay profiles of H_2O_2 at both pH values were indistinguishable, thus confirming that the reactivity of H_2O_2 towards bare ZVI (Eq. (7)) is rather independent of the working pH. Moreover, as the rate of H_2O_2 consumption through Fenton processes is rather low in circumneutral media, the comparison of the profiles obtained in the presence of *o*-phenantrholine with the one obtained at pH_i 5 in additive-free conditions suggests that the presence of the corrosion layer only decreases the reactivity of ZVI towards H_2O_2 by a factor of less than 2.

On the other hand, in the presence of EDTA the H_2O_2 consumption profiles were very similar to the one observed at pH_i 3 in the absence of additives. The latter results can be rationalized by considering the fact that EDTA not only disturbs the structure of the CL but also allows the Fenton reaction, thus making Eq. (1) an important H_2O_2 consumption pathway at both pH values.

3.4.2. Addition of radical scavengers

2-propanol is a well-known HO· radical scavenger frequently used to assess the nature of the oxidant produced both in Fenton and ZVI systems [8–10], while DMSO is capable of scavenging not only HO· radicals but also less reactive species such as ferryl ions (FeO^{2+}) [9]. Experiments performed with added 2-propanol (0.5 M) at pH_i 3 showed an inhibition of AB1 decolorization higher than 98% (Fig. 6), thus confirming that oxidative transformation of AB1 in acidic media is essentially driven by HO· radicals. In contrast, the addition of 2-propanol at pH_i 5 exerted a much less important effect on AB1 decolorization, with an inhibition of around 57% (Fig. 6b).

Since oxidative transformations at circumneutral pH values may involve the participation of alternative oxidants such as FeO^{2+} [8–10], additional experiments were performed in the presence of DMSO at pH_i 5. The results obtained showed practically the same AB1 decolorization profile in the presence of either 2-propanol or DMSO, suggesting that

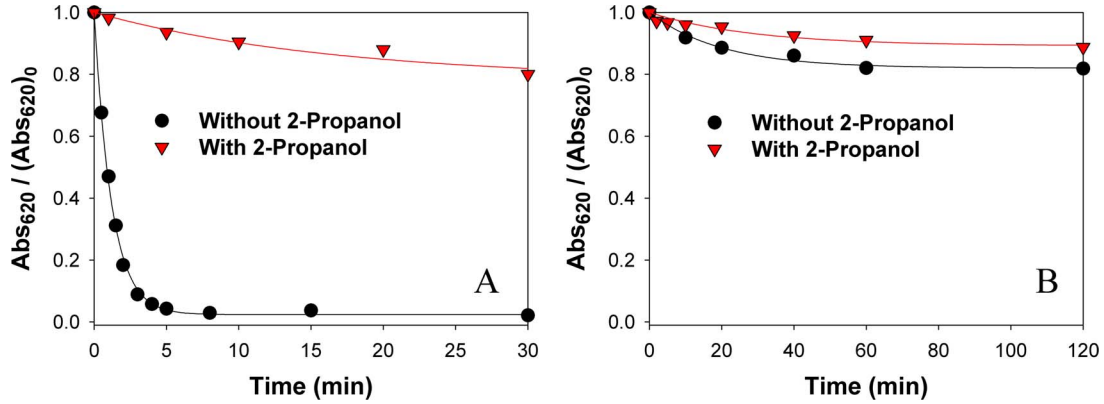

Fig. 6. Effect of addition of 2-propanol on AB1 decolorization in ZVI/O_2/H_2O_2 systems. (A) pH 3.00 (B) pH 5.00. Conditions: $[AB1]_0 = 50\ mg\ L^{-1}$, $[H_2O_2]_0 = 0.5\ mM$, $[Na_2SO_4]_0 = 5.0\ mM$, [2-propanol] = 0.5 M.

the residual decolorization (of about 43%) is essentially related to reductive transformation pathways rather than to the participation of oxidants different from HO·. Moreover, kinetic profiles obtained with added 2-propanol (Fig. 6) allow estimating the initial rates of AB1 decolorization through purely reductive pathways. Interestingly, the analysis reveals that the rate of surface-mediated AB1 reductive transformation only decreases by a factor of 3.3 as pH_i is raised from 3 to 5.

Finally, the comparison between the estimated rate of AB1 decolorization through oxidative pathways recorded at pH_i 5 (i.e., about 57% of the decay rate in Fig. 6b without 2-propanol) and the overall rate of H_2O_2 consumption under the same conditions (i.e., the decay in Fig. 5 for pH_i 5 without additives) shows that H_2O_2 consumption rate is at least 25 faster than the rate of AB1 oxidative decolorization. The latter values suggest that at circumneutral pH values more than 96% of the added oxidant is not involved in AB1 decolorization but depleted through sacrificial processes, Eq. (7) being the dominant one.

3.5. Analysis of TOC evolution and toxicity measurements

The profiles of Total Organic Carbon were recorded under different conditions (Fig. S10, Sup. Info.). Results showed no variation during the timescales analyzed for the ZVI/N_2 experiments, demonstrating that solution decolorization does not involve adsorption processes of AB1 or its products of reductive transformation. In contrast, TOC reductions of about 35% were observed in ZVI/O_2/H_2O_2 systems, thus suggesting that processes such as adsorption of AB1 oxidation by-products on ZVI surface and chemical reactions which release CO_2 may take place under oxidative conditions.

The toxicity of AB1 solutions treated by ZVI/N_2 or ZVI/O_2/H_2O_2 systems was analyzed according to the inhibition of the luminescence of *V. fischeri* bacteria. For $50\ mg\ L^{-1}$ of AB1 a 10% inhibition of luminescence was measured. During ZVI/N_2 treatment, toxicity increased with time and reached an inhibition of luminescence of 50% after 2 h (Fig. S11, Sup Info). This is consistent with formation of aniline and *p*-nitroaniline among the main reaction products, since it has been reported by Chang et al. [24] that aromatic amines produced are more toxic than AB1. Therefore, purely reductive transformations are not advisable due to the increase of toxicity with the reaction progress.

On the other hand, the analysis of toxicity in ZVI/O_2/H_2O_2 systems shows a more complex scenario. Because of the presence of H_2O_2 during the first stages of AB1 degradation, toxicity values cannot be straightforward correlated with the organic composition of the reaction mixtures. Therefore, in order to avoid the interference of H_2O_2, toxicity analyses were performed at 40 min (i.e., after complete exhaustion of H_2O_2). Different oxidation degrees were achieved by varying the initial concentration of added oxidant from 0.1 to 0.9 mM. Luminescence inhibition remained below 20% despite the relatively low initial H_2O_2 concentrations tested (data not shown), thus indicating that oxidative pathways are rather efficient for limiting the toxicity increase of treated solutions. The latter results may be explained by taking into account that, in the presence of H_2O_2, aromatic amines resulting from AB1 reductive pathways may be further transformed into less toxic compounds by $HO^{\bullet}$ radical-induced oxidations [49].

4. Conclusions

ZVI-assisted Fenton systems usually exhibit strong pH dependent kinetics. The results here presented show that, for substrates bearing reducible groups, the relative contributions of reductive and oxidative pathways are also significantly pH-dependent due to the interplay of several competitive processes. For the model azo compound studied, the investigation of reaction rates under different conditions allowed a quantitative discussion concerning the key steps that govern the transformation mechanism. In acidic media the fast AB1 decolorization predominantly occurs (> 98%) via oxidative pathways triggered by HO · radicals produced through the Fenton reaction, whereas in circumeutral media the much slower AB1 transformation involves both oxidative (57%) and reductive (43%) pathways. The latter proportions are in turn ruled by the dominant H_2O_2 consumption pathway. In acidic media, a fairly high proportion (89%) of H_2O_2 consumption is linked to Fenton processes due to the high concentrations of soluble Fe(II) released to the aqueous phase. In contrast, given the scarce production of $Fe(II)_{aq}$ in circumneutral media, H_2O_2 consumption is largely decoupled from AB1 decolorization and mostly (> 96%) related to processes involving ZVI particles.

Since the availability of aqueous Fe(II) is a key parameter for ZVI-assisted Fenton systems, assessing which factors determine its behavior as pH_i is shifted from 3 to 5 is of major importance. A reasonable and frequently assumed explanation is that the increase of pH favors the growth of a thick corrosion layer onto ZVI particles which significantly lowers their reactivity. However, according to the results here presented, this explanation is not completely satisfactory since the corrosion layer only moderately decreases (a factor of about 3) the overall rates of H_2O_2, H^+ and AB1 reduction through heterogeneous processes. The latter behavior cannot be straightforward associated with the large decrease (a factor of about 240) in the rate of Fe(II) released into the aqueous phase. Noteworthy, Fe(II) species are fairly soluble in the studied pH range but the solubility of Fe(III) species is significantly decreased as pH_i is increased from 3 to 5. Hence, the large difference between ZVI corrosion rate and $Fe(II)_{aq}$ release rate may be explained by considering that, for ZVI/O_2/H_2O_2 systems operated at pH_i 5, before leaving the particles surface an important fraction of Fe(II) species produced by Fe(0) oxidation is further transformed to Fe(III) species and precipitates. In this context, the results suggest that as pH_i is increased from 3 to 5, the mechanism of Fe(II) oxidation shifts from a reaction mediated by H_2O_2 (Eq. (1)) to a mixed mechanism that also

involves an important contribution of dissolved oxygen mediated heterogeneous processes (Eq. (16)).

Acknowledgements

The present work was partially supported by UNLP (11/X679), ANPCyT (PICT-2012-0423, PICT-2015-0374) and CONICET (PIP: 12-2013-01-00236CO). Authors also want to acknowledge the economic support of European Union Call: (H2020-MSCA-RISE-2014, Proyect 645551 (MAT4TREAT). A. Arques and L. Carlos want to acknowledge Spanish Ministerio de Economía y Competividad (CTQ2015-69832, Triceratops Project). A. Donadelli thank the CONICET for his research graduate grant. L. Carlos and F. S. García Einschlag are research members of CONICET.

Appendix A. Supplementary data

Supplementary material related to this article can be found, in the online version, at doi:https://doi.org/10.1016/j.apcatb.2018.02.057.

References

[1] Y. He, J.F. Gao, F.Q. Feng, C. Liu, Y.Z. Peng, S.Y. Wang, The comparative study on the rapid decolorization of azo, anthraquinone and triphenylmethane dyes by zero-valent iron, Chem. Eng. J. 179 (2012) 8–18, http://dx.doi.org/10.1016/j.cej.2011.05.107.

[2] P.V. Nidheesh, R. Gandhimathi, S.T. Ramesh, Degradation of dyes from aqueous solution by Fenton processes: a review, Environ. Sci. Pollut. Res. 20 (2013) 2099–2132, http://dx.doi.org/10.1007/s11356-012-1385-z.

[3] J. Fan, Y. Guo, J. Wang, M. Fan, Rapid decolorization of azo dye methyl orange in aqueous solution by nanoscale zerovalent iron particles, J. Hazard. Mater. 166 (2009) 904–910, http://dx.doi.org/10.1016/j.jhazmat.2008.11.091.

[4] K. Othmer, Dyes, environmental chemistry, in: Watcher (Ed.), Encycl. Chem. Technol. 4th ed., Wiley-Interscience, New York, 1998, , http://dx.doi.org/10.1021/ja9857662 p. 932.

[5] S. Nam, P.G. Tratnyek, Reduction of azo dyes with zero-valent iron, Water Res. 34 (2000) 1837–1845, http://dx.doi.org/10.1016/S0043-1354(99)00331-0.

[6] J.J. Pignatello, E. Oliveros, A. MacKay, Advanced oxidation processes for organic contaminant destruction based on the fenton reaction and related chemistry, Crit. Rev. Environ. Sci. Technol. 36 (2006) 1–84, http://dx.doi.org/10.1080/10643380500326564.

[7] F.S.G. Einschlag, A.M. Braun, E. Oliveros, Fundamentals and applications of the photo-fenton process to water treatment, in: D. Bahnemann, P. Robertson (Eds.), Environ. Photochem. Part III, 2013, http://dx.doi.org/10.1007/698.

[8] I.A. Katsoyiannis, T. Ruettimann, S.J. Hug, pH dependence of fenton reagent generation and As(III) oxidation and removal by corrosion of zero valent iron in aerated water, Environ. Sci. Technol. 42 (2008) 7424–7430, http://dx.doi.org/10.1021/es800649p.

[9] C.R. Keenan, D.L. Sedlak, Factors affecting the yield of oxidants from the reaction of nanoparticulate zero-valent iron and oxygen, Environ. Sci. Technol. 42 (2008) 1262–1267, http://dx.doi.org/10.1021/es7025664.

[10] C.R. Keenan, D.L. Sedlak, Ligand-enhanced reactive oxidantgeneration by nanoparticulate zero-valent iron and oxygen, Environ. Sci. Technol. 42 (2008) 6936–6941, http://dx.doi.org/10.1021/es801438f%0A.

[11] C. Noubactep, Investigating the processes of contaminant removal in Fe0/H2O systems, Korean J. Chem. Eng. 29 (2012) 1050–1056, http://dx.doi.org/10.1007/s11814-011-0298-8.

[12] C. Noubactep, A critical review on the process of contaminant removal in Fe0–H2O systems, Environ. Technol. 29 (2008) 909–920, http://dx.doi.org/10.1080/09593330802131602.

[13] J. Wang, J. Farrell, Investigating the role of atomic hydrogen on chloroethene reactions with iron using Tafel analysis and electrochemical impedance spectroscopy, Environ. Sci. Technol. 37 (2003) 3891–3896, http://dx.doi.org/10.1021/es0264605.

[14] V. Jovancicevic, J.O.M. Bockris, The mechanism of oxygen reduction on iron in neutral solutions, J. Electrochem. Soc. 133 (1986) 1797–1807, http://dx.doi.org/10.1149/1.2109021.

[15] C. Noubactep, Processes of contaminant removal in “Fe0-H2O” systems revisited: the importance of co-precipitation, Open Environ. Sci. 1 (2007) 9–13, http://dx.doi.org/10.1080/09593330802131602.

[16] X. Guo, Z. Yang, H. Liu, X. Lv, Q. Tu, Q. Ren, X. Xia, C. Jing, Common oxidants activate the reactivity of zero-valent iron (ZVI) and hence remarkably enhance nitrate reduction from water, Sep. Purif. Technol. 146 (2015) 227–234, http://dx.doi.org/10.1016/j.seppur.2015.03.059.

[17] Y.H. Huang, T.C. Zhang, Effects of dissolved oxygen on formation of corrosion products and concomitant oxygen and nitrate reduction in zero-valent iron systems with or without aqueous Fe2+, Water Res. 39 (2005) 1751–1760, http://dx.doi.org/10.1016/j.watres.2005.03.002.

[18] K.V.K. Ansaf, S. Ambika, I.M. Nambi, Performance enhancement of zero valent iron based systems using depassivators: optimization and kinetic mechanisms, Water Res. 102 (2016) 436–444, http://dx.doi.org/10.1016/j.watres.2016.06.064.

[19] C.H. Weng, Y.T. Lin, H.M. Yuan, Rapid decoloration of Reactive Black 5 by an advanced Fenton process in conjunction with ultrasound, Sep. Purif. Technol. 117 (2013) 75–82, http://dx.doi.org/10.1016/j.seppur.2013.03.047.

[20] C.H. Weng, Y.T. Lin, C.K. Chang, N. Liu, Decolourization of direct blue 15 by Fenton/ultrasonic process using a zero-valent iron aggregate catalyst, Ultrason. Sonochem. 20 (2013) 970–977, http://dx.doi.org/10.1016/j.ultsonch.2012.09.014.

[21] L. Santos-juanes, F.S.G. Einschlag, A.M. Amat, A. Arques, Combining ZVI reduction with photo-Fenton process for the removal of persistent pollutants, Chem. Eng. J. 310 (2016) 484–490, http://dx.doi.org/10.1016/j.cej.2016.04.114.

[22] C. He, J. Yang, L. Zhu, Q. Zhang, W. Liao, S. Liu, Y. Liao, M.A. Asi, D. Shu, pH-dependent degradation of acid orange II by zero-valent iron in presence of oxygen, Sep. Purif. Technol. 117 (2013) 59–68, http://dx.doi.org/10.1016/j.seppur.2013.04.028.

[23] R.C. Martins, D.V. Lopes, M.J. Quina, R.M. Quinta-Ferreira, Treatment improvement of urban landfill leachates by Fenton-like process using ZVI, Chem. Eng. J. 192 (2012) 219–225, http://dx.doi.org/10.1016/j.cej.2012.03.053.

[24] S.-H. Chang, S.-H. Chuang, H.-C. Li, H.-H. Liang, L.-C. Huang, Comparative study on the degradation of I.C. Remazol Brilliant Blue R and I.C. Acid Black 1 by Fenton oxidation and Fe0/air process and toxicity evaluation, J. Hazard. Mater. 166 (2009) 1279–1288, http://dx.doi.org/10.1016/j.jhazmat.2008.12.042.

[25] W.J. Epolito, H. Yang, L.A. Bottomley, S.G. Pavlostathis, Kinetics of zero-valent iron reductive transformation of the anthraquinone dye Reactive Blue 4, J. Hazard. Mater. 160 (2008) 594–600, http://dx.doi.org/10.1016/j.jhazmat.2008.03.033.

[26] X. Fan, X. Guan, J. Ma, H. Ai, Kinetics and corrosion products of aqueous nitrate reduction by iron powder without reaction conditions control, J. Environ. Sci. 21 (2009) 1028–1035, http://dx.doi.org/10.1016/S1001-0742(08)62378-5.

[27] L. Carlos, D. Fabbri, A.L. Capparelli, A.B. Prevot, E. Pramauro, F.S.G. Einschlag, Intermediate distributions and primary yields of phenolic products in nitrobenzene degradation by Fenton’s reagent, Chemosphere 72 (2008) 952–958, http://dx.doi.org/10.1016/j.chemosphere.2008.03.042.

[28] W. Sung, J.J. Morgan, Kinetics and product of ferrous iron oxygenation in aqueous systems, Environ. Sci. Technol. 14 (1980) 561–568, http://dx.doi.org/10.1021/es60165a006.

[29] J. Ashworth, E. Nijenhuis, B. Glowacka, L. Tran, L. Schenck-Watt, Turbidity and Color Correction in the Microto Bioassay, Open Environ. Pollut. Toxicol. J. 2 (2010) 1–7, http://dx.doi.org/10.2174/1876397901002010001.

[30] J. Sun, S. Sun, G. Wang, L. Qiao, Degradation of azo dye Amido black 10B in aqueous solution by Fenton oxidation process, Dyes Pigm. 74 (2007) 647–652, http://dx.doi.org/10.1016/j.dyepig.2006.04.006.

[31] L.J. Matheson, P.G. Tratnyek, Reductive Dehalogenation of chlorinated Methanes by iron metal, Environ. Sci. Technol. 28 (1994) 2045–2053, http://dx.doi.org/10.1021/es00061a012.

[32] A. Agrawal, P.G. Tratnyek, Reduction of nitro aromatic compounds by zero-valent iron metal, Environ. Sci. Technol. 30 (1996) 153–160, http://dx.doi.org/10.1021/es950211h.

[33] K. Krapfenbauer, H. Wolfger, N. Geto, I. Hamblett, S. Navaratnam, Pulse radiolysis and chemical analysis of azo dyes in aqueous solution I. p-phenylazoaniline, Radiat. Phys. Chem. 58 (2000) 21–27, http://dx.doi.org/10.1016/S0969-806X(99)00356-4.

[34] J.T. Spadaro, L. Isabelle, V. Renganathan, Hydroxyl radical mediated degradation of azo dyes: evidence for benzene generation, Environ. Sci. Technol. 28 (1994) 1389–1393, http://dx.doi.org/10.1021/es00056a031.

[35] A.S. Özen, V. Aviyente, R.A. Klein, Modeling the oxidative degradation of azo dyes: a density functional theory study, J. Phys. Chem. A 107 (2003) 4898–4907, http://dx.doi.org/10.1021/jp026287z.

[36] S. Hisaindee, M.A. Meetani, M.A. Rauf, Application of LC-MS to the analysis of advanced oxidation process (AOP) degradation of dye products and reaction mechanisms, TrAC - Trends Anal. Chem. 49 (2013) 31–44, http://dx.doi.org/10.1016/j.trac.2013.03.011.

[37] M.A. Meetani, M.A. Rauf, S. Hisaindee, A. Khaleel, A. AlZamly, A. Ahmad, Mechanistic studies of photoinduced degradation of Orange G using LC/MS, RSC Adv. 1 (2011) 490, http://dx.doi.org/10.1039/c1ra00177a.

[38] M.A. Meetani, S.M. Hisaindee, F. Abdullah, S.S. Ashraf, M.A. Rauf, Liquid chromatography tandem mass spectrometry analysis of photodegradation of a diazo compound: a mechanistic study, Chemosphere 80 (2010) 422–427, http://dx.doi.org/10.1016/j.chemosphere.2010.04.065.

[39] W. Yin, J. Wu, P. Li, X. Wang, N. Zhu, P. Wua, B. Yang, Experimental study of zero-valent iron induced nitrobenzene reduction in groundwater: the effects of pH, iron dosage, oxygen and common dissolved anions, Chem. Eng. J. 184 (2012) 198–204, http://dx.doi.org/10.1016/j.cej.2012.01.030.

[40] W.F. Wüst, R. Köber, O. Schlicker, A. Dahmke, Combined zero- and first-order kinetic model of the degradation of tce and cis-DCE with commercial iron, Environ. Sci. Technol. 33 (1999) 4304–4309, http://dx.doi.org/10.1021/es980439f.

[41] J.M. Triszcz, A. Porta, F.S. García Einschlag, Effect of operating conditions on iron corrosion rates in zero-valent iron systems for arsenic removal, Chem. Eng. J. 150 (2009) 431–439, http://dx.doi.org/10.1016/j.cej.2009.01.029.

[42] L.G. Devi, K.E. Rajashekhar, K.S.A. Raju, S.G. Kumar, Kinetic modeling based on the non-linear regression analysis for the degradation of Alizarin Red S by advanced photo Fenton process using zero valent metallic iron as the catalyst, J. Mol. Catal. A Chem. 314 (2009) 88–94, http://dx.doi.org/10.1016/j.molcata.2009.08.021.

[43] J.A. de Lima Perini, R. Fernandes Pupo Nogueira, Zero-valent iron mediated degradation of sertraline - effect of H2O2 addition and application to sewage treatment plant effluent, J. Chem. Technol. Biotechnol. 91 (2016) 276–282, http://dx.

doi.org/10.1002/jctb.4705.
[44] D.M. Cwiertny, A.L. Roberts, On the nonlinear relationship between kobs and reductant mass loading in iron batch systems, Environ. Sci. Technol. 39 (2005) 8948–8957, http://dx.doi.org/10.1021/es050472j.
[45] C. Noubactep, Characterizing the effects of shaking intensity on the kinetics of metallic iron dissolution in EDTA, J. Hazard. Mater. 170 (2009) 1149–1155, http://dx.doi.org/10.1016/j.jhazmat.2009.05.085.
[46] J.H. Fan, H.W. Wang, D.L. Wu, L.M. Ma, Effects of electrolytes on the reduction of 2,4-dinitrotoluene by zero-valent iron, J. Chem. Technol. Biotechnol. 85 (2010) 1117–1121, http://dx.doi.org/10.1002/jctb.2407.
[47] B. Morgan, O. Lahav, The effect of pH on the kinetics of spontaneous Fe(II) oxidation by O2 in aqueous solution - basic principles and a simple heuristic description, Chemosphere 68 (2007) 2080–2084, http://dx.doi.org/10.1016/j.chemosphere.2007.02.015.
[48] L. Nassi-Calo, C. Mello-Filho, R. Meneghini, O-Phenanthroline protects mammalian cells from hydrogen peroxide-induced Gene mutation and morphological transformation, Carcinogenesis. 10 (1989) 1055–1057, http://dx.doi.org/10.1093/carcin/10.6.1055.
[49] M. Fukushima, K. Tatsumi, K. Morimoto, The fate of aniline after a photo-fenton reaction in an aqueous system containing iron (III), humic acid, and hydrogen peroxide, Environ. Sci. Technol. 34 (2000) 2006–2013, http://dx.doi.org/10.1021/es991058k.